Commensurate-commensurate phase transitions induced by an external magnetic field in spin Hamiltonians with continuous symmetry

1994 J. Phys.: Condens. Matter 6 2499

(http://iopscience.iop.org/0953-8984/6/13/011)

J. Phys.: Condens. Matter 6 (1994) 2499–2510. Printed in the UK

Commensurate–commensurate phase transitions induced by an external magnetic field in spin Hamiltonians with continuous symmetry

E Rastelli, S Sedazzari and A Tassi
Dipartimento di Fisica dell'Universitá, 43100 Parma, Italy

Received 11 October 1993, in final form 10 January 1994

Abstract. Commensurate–commensurate phase transitions are known to occur in the Ising model with competing interactions (ANNNI model). We show that an analogous scenario may occur in spin Hamiltonians with continuous symmetry and competing interactions when an external magnetic field is applied. In particular we study a planar square lattice with exchange competition up to third neighbours. We consider exchange competition suitable for giving a zero-temperature–zero-field configuration characterized by a spin–spin turn angle $Q = 4\pi/5$. In contrast with previous conclusions, based on the hypothesis that the unit magnetic cell does not change under the effect of an external magnetic field, we find discontinuous phase transitions between a distorted-helix phase (with five spins per cell) and the spin-flop phase (with two spins per cell) and between the spin-flop phase and a fan phase (with five spins per cell). This behaviour seems to be a general rule for large enough Q as confirmed by the helix with a turn angle $Q = 6\pi/7$ in zero field.

1. Introduction

A sequence of different commensurate spin configurations is established by suitable exchange competition in the axial next-nearest-neighbour Ising (ANNNI) model [1]. Non-simple spin configurations are also found in simple spin Hamiltonians with continuous symmetry such as the planar and Heisenberg model. This scenario is caused by either a sufficiently strong exchange competition [2] or the lattice structure [3]. Note that for classical models helix spin configurations exhaust the minimum-energy configurations [4]. The scenario is even richer when an external magnetic field is applied because of the competition between the field, which favours a collinear configuration, and the frustration, which favours a helix configuration. Frustration can be induced by competing exchange interactions or by the lattice structure as occurs in triangular, hexagonal, and rhombohedral antiferromagnets [3]. In both cases a number of well grounded results has been achieved. An exact low-temperature–low-field expansion of the free energy [5] for the planar model shows that helix configurations commensurate with the underlying lattice are locked by non-analytic delta-like contributions proportional to H^p where H is the external magnetic field and p is the number of spins per unit magnetic cell. Minimization of the zero-temperature energy under the hypothesis that the magnetic cell is unaffected by the field [6] suggests a first-order phase transition between the low-field (distorted-helix) phase and the high-field (fan) configuration when the zero-field spin–spin turn angle Q is less than $\pi/2$, whereas a continuous distortion of the helix into the fan is suggested for $Q > \pi/2$. This picture seems to be supported by the exact solution of the planar linear chain in an external magnetic

0953-8984/94/132499+12$19.50

field obtained by the transfer matrix method [7] and by Monte Carlo (MC) simulations on the planar (finite size) square lattice [6, 8]. However, the calculation of the elementary excitation energies for competing interactions that stabilize a helix with a spin–spin turn angle $Q = 4\pi/5$ at zero field undergoes unexpected instabilities. Indeed one branch of the excitation energy softens in the neighbourhood of the zone-boundary wave vector for a wide range of applied magnetic fields. This is the signature of the onset of a new commensurate configuration with two spins per unit magnetic cell. Indeed we have found that for a finite range of fields $H_1 < H < H_2$ the spin-flop phase has an energy lower than both the distorted helix and fan configurations. Moreover the elementary excitations in the spin-flop phase are well defined in that range of fields. In order to test whether this scenario is a general rule for *any* Q close to π we have studied the minimum energy configuration for an exchange competition that supports a commensurate helix with $Q = 6\pi/7$ in zero magnetic field. We find also in this case distorted-helix, spin-flop, and fan configurations connected by first-order phase transitions.

We revise our previous conclusions based on analytic calculations at zero temperature with the hypothesis of a fixed magnetic cell, as well as numerical results at finite temperature, where no evidence of any phase transition between spin configurations with different commensurate magnetic cells was found for $Q > \pi/2$ [6, 7]. We realize that this is probably due to the the low temperature range in which the transitions occur. Note that even at zero temperature the magnetization discontinuities at the transitions are very weak. It is well known that both the numerical solution of the transfer matrix integral equation for the linear chain [7] and the MC simulation for the square lattice [6, 8] become unreliable at very low temperature. On the other hand, in the temperature range where the numerical methods are efficient the trace of discontinuous helix–spin-flop and spin-flop–fan phase transitions is hardly recognizable. Instead of looking at the magnetization, which undergoes weak discontinuities at the transitions, we think that the static structure factor is a more sensible probe. Indeed when the distorted helix–spin-flop transition occurs a peak at $q = (4\pi/5, 0)$ disappears and a peak at $q = (\pi, 0)$ appears. These peaks, however, are broad in 1D [7] where thermal fluctuations severely affect them. Early MC simulations on samples of 25×25 spins with periodic boundary conditions [6] did not show any new peak at $q = (\pi, 0)$ in the static structure factor at increasing magnetic field as one would expect if the spin-flop phase intervened. However, the reason has to be traced back to the bad choice of sample dimensions, which were not suitable for allowing dimerization of the spin patterns. Therefore, we have considered samples of 50×50 spins and transition between an ordered phase with five spins per cell singled out by a peak at $q = (4\pi/5, 0)$ in the static structure factor, and a spin-flop phase characterized by a peak at $q = (\pi, 0)$ has been recognized.

In section 2 we compare the energies of the various configurations evaluated analytically for $Q = 4\pi/5$ and $Q = 6\pi/7$. We give the elementary excitation energies of the various stable phases for $Q = 4\pi/5$. In section 3 we give the finite-temperature thermodynamics obtained by numerical results from MC simulations. Section 4 contains a summary and conclusions.

2. Distorted-helix, symmetric fan and spin-flop phases

We consider a planar square model with nearest-neighbour ferromagnetic coupling $2J_1 > 0$, next-nearest-neighbour coupling $2J_2$, and third-nearest-neighbour coupling $2J_3$. The model Hamiltonian reads

$$\mathcal{H} = -J_1 \sum_{i,\delta_1} \boldsymbol{S}_i \cdot \boldsymbol{S}_{i+\delta_1} - J_2 \sum_{i,\delta_2} \boldsymbol{S}_i \cdot \boldsymbol{S}_{i+\delta_2} - J_3 \sum_{i,\delta_3} \boldsymbol{S}_i \cdot \boldsymbol{S}_{i+\delta_3} - \mu \sum_i \boldsymbol{H} \cdot \boldsymbol{S}_i \qquad (2.1)$$

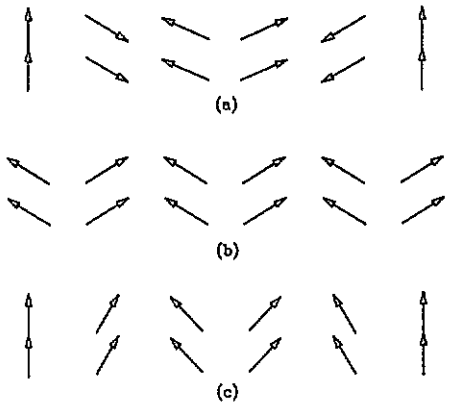

Figure 1. (a) A unit magnetic cell with five spins suitable for describing the distorted-helix phase with $h = h_1 = 0.334$; (b) the spin-flop phase for $h = 1$; (c) the symmetric-fan phase for $h = h_2 = 1.419$.

where S_i is a two-component unit vector and μ is the magnetic moment per lattice spin. The zero-temperature–zero-field phase diagram in the plane spanned by the reduced exchange couplings $j_2 = J_2/J_1$ and $j_3 = J_3/J_1$ is shown in figure 1 of reference [2]. We focus on the line $1 + 2j_2 = -4j_3 \cos(4\pi/5)$, where the minimum-energy configuration is a regular helix characterized by a wave vector $Q = (4\pi/5, 0)$. This commensurate helix configuration with five spins per unit cell is expected to be unaffected by the field [5], at least in the low-field range. Under this assumption a direct calculation of the minimum energy configuration can be performed for any field. Indeed the square lattice can be divided into five sublattices, each spin of which makes an angle ϕ_s ($s = 1, ..., 5$) with the external applied field. The minimum-energy configuration is then obtained by looking for the minimum of this function with respect to ϕ_s. The solution is a minimum-energy configuration with one spin of the unit cell parallel to the field and the other four spins symmetrically oriented with respect to the field. For instance, $\phi_1 = 0$, $\phi_2 = -\phi_5$, $\phi_3 = -\phi_4$, where ϕ_2 and ϕ_3 are solutions of the following system:

$$(1 + 2j_2)[\sin\phi_2 + \sin(\phi_2 - \phi_3)] + j_3[\sin(\phi_2 + \phi_3) + \sin(2\phi_2)] + h\sin\phi_2 = 0 \tag{2.2}$$

$$(1 + 2j_2)[\sin(2\phi_3) + \sin(\phi_3 - \phi_2)] + j_3[\sin(\phi_3 + \phi_2) + \sin\phi_3] + h\sin\phi_3 = 0 \tag{2.3}$$

where $h = \mu H/2J_1$. The stable configurations given by (2.2) and (2.3) are shown in figure 1(a) (distorted-helix phase) and in figure 1(c) (fan phase). A similar calculation was performed on the Hamiltonian (2.1) for competing interactions leading to a helix wave vector $Q = (2\pi/5, 0)$ at zero field [8]. In that case a first-order phase transition between the distorted helix and the fan phase was found. In contrast with such a result no first-order helix–fan transition is found from (2.2) and (2.3) in the present calculation for $Q = 4\pi/5$. The change from the distorted helix to the fan configuration and, finally, to the saturated phase (reached at $h_s = -4j_3 \cos 4\pi/5$) occurs in a continuous way. The reduced energy of the above configurations as obtained from (2.2) and (2.3) is

$$e_0^{(H)} = \frac{E_0^{(H)}}{2J_1N} = -\frac{1}{5}\Big\{(1 + 2j_2)[2\cos\phi_2 + 2\cos(\phi_2 - \phi_3) + \cos(2\phi_3)] + 5(1 + j_3) + j_3[2\cos\phi_3 + 2\cos(\phi_2 + \phi_3) + \cos(2\phi_2)] + h(1 + 2\cos\phi_2 + 2\cos\phi_3)\Big\} \tag{2.4}$$

This zero-temperature result, supported by numerical calculations performed at finite temperature on the linear chain [7] and on the square lattice [6, 8], led us to the conclusion that no first-order phase transition occurs when the exchange competition supports spin helices with Q large enough. However, if we evaluate the elementary excitation energies accounting for small deviations away from the minimum energy configuration in Hamiltonian (2.1), unexpected results are obtained. For the choice $j_3 = -0.125$, $j_2 = -0.702\,25$ the lowest branch of the elementary excitation energy becomes negative about the zone-boundary wave vector $q = (\pi/5, 0)$ over a wide range of magnetic fields ($0.83 < h < 1.37$) even though (2.4) is a minimum with respect to ϕ_s. The instability of the elementary excitation energies for $0.83 < h < 1.37$, singled out by a softening of a branch in the vicinity of the zone boundary, suggests that the actual minimum energy configuration in that range of fields has to be looked for in the manifold of dimerized phases such as, for instance, the spin-flop phase. In any case the configuration with five spins per unit cell is not preserved over the whole range of magnetic fields. Assuming a spin-flop configuration where the spins make an angle ϕ with respect to the external magnetic field as shown in figure 1(b), the energy one obtains from Hamiltonian (2.1) is

$$e_0^{(SF)} = \frac{E_0^{(SF)}}{2J_1N} = -1 - \cos(2\phi) - 2j_2\cos(2\phi) - 2j_3 - h\cos\phi \tag{2.5}$$

with

$$\cos\phi = -\frac{h}{4(1+2j_2)}. \tag{2.6}$$

Table 1 gives $e_0^{(H)}$ and $e_0^{(SF)}$ as function of h for $j_3 = -0.125$ on the line $1 + 2j_2 = -4j_3\cos 4\pi/5$. As one can see the spin-flop phase is stable in the range $h_1 < h < h_2$, where $h_1 = 0.334$ ($e_0^{(H)} = e_0^{(SF)} = -1.188\,984$) and $h_2 = 1.419$ ($e_0^{(H)} = e_0^{(SF)} = -1.776\,664$). The zero temperature uniform magnetization of the two phases is obtained by the usual thermodynamic relation $m_0 = -(1/\mu N)\partial E_0/\partial H$. From (2.4) and (2.5) one obtains

$$m_0^{(H)} = \tfrac{1}{5}(1 + 2\cos\phi_2 + 2\cos\phi_3) \tag{2.7}$$

and

$$m_0^{(SF)} = \cos\phi. \tag{2.8}$$

The magnetization as a function of the field is shown by the continuous curve of figure 2. The helix–spin-flop and spin-flop–fan phase transitions are discontinuous even though the jumps in the magnetization are very small ($\Delta m = 0.048$ at $h = h_1$, and $\Delta m = 0.010$ at $h = h_2$). The distorted helix, spin-flop, and fan phases are illustrated in figure 1. In order to test the stability of the spin-flop phase we have evaluated the elementary excitation energies of this phase and we have proved that they are positive over the range $0.192 < h < 1.607$, which is wider than the range $0.334 < h < 1.419$ where the spin-flop phase is stable. In the appendix details of the calculation of the elementary excitation energy for both the phase with five spins per cell and the spin-flop phase are given. The excitation energies of these phases are shown in figures 3 and 4 for selected values of the field.

The static structure factor is much more affected than the magnetization by the transition because of a different location of the Bragg peaks in the helix and spin-flop phases. Moreover the intensity of the peak changes under the effect of an external magnetic field.

Table 1. A comparison between the energy ($e_0^{(H)}$) of the helix phase with five spins per unit cell and the energy ($e_0^{(SF)}$) of the spin-flop phase as a function of the external magnetic field for $j_3 = -\frac{1}{8}$.

h	$e_0^{(H)}$	$e_0^{(SF)}$
0	−1.163 627	−1.154 508
0.1	−1.165 841	−1.157 600
0.2	−1.172 534	−1.166 869
0.3	−1.183 938	−1.182 320
0.4	−1.200 662	−1.203 951
0.5	−1.223 759	−1.231 763
0.6	−1.254 294	−1.265 755
0.7	−1.292 821	−1.305 927
0.8	−1.339 307	−1.352 279
0.9	−1.393 350	−1.404 812
1.0	−1.454 413	−1.463 525
1.1	−1.521 982	−1.528 419
1.2	−1.595 634	−1.599 493
1.3	−1.675 045	−1.676 747
1.4	−1.759 985	−1.760 182
1.5	−1.850 286	−1.849 797
1.6	−1.945 830	−1.945 592
1.6363	−1.981 763	−1.981 763

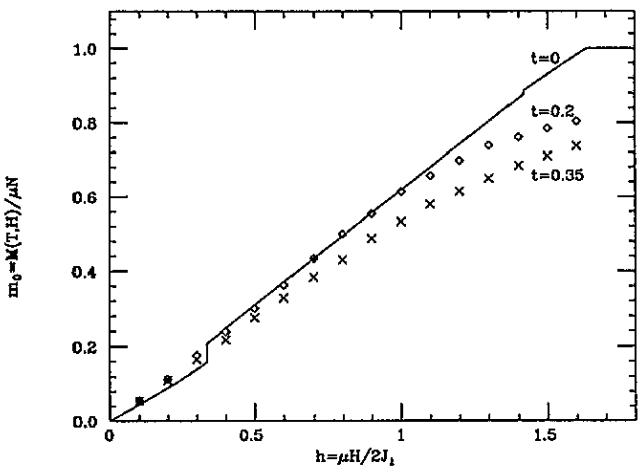

Figure 2. The magnetization versus the magnetic field for $j_3 = -\frac{1}{8}$: the analytic result at $T = 0$ (continuous curve); MC simulation at $T = 0.2$ (diamonds) and $T = 0.35$ (crosses).

The static structure factor, which is the spatial Fourier transform of the static correlation function, is

$$S(q) = \frac{1}{N^2} \sum_{ij} e^{iq\cdot(r_i - r_j)} \cos(\phi_i - \phi_j). \tag{2.9}$$

At $T = 0$, in the helix phase (five spins per cell) (2.9) reads

$$S(q_x, q_y) = \delta(q_x - \frac{2\pi}{5}m)\delta(q_y - 2\pi n)\frac{1}{25}\left\{5 + 2\cos q_x\left[\cos\phi_2 + 2\cos(\phi_2 - \phi_3) + \cos(2\phi_3)\right]\right.$$

$$+ 2\cos(2q_x)\big[\cos\phi_3 + 2\cos(\phi_2 + \phi_3)\big]$$
$$+ 2\cos(3q_x)\big[\cos\phi_3 + \cos(2\phi_2)\big] + 2\cos(4q_x)\cos\phi_2\Big\} \tag{2.10}$$

with ϕ_2 and ϕ_3 given by (2.2) and (2.3). In the spin-flop phase (2.9) becomes

$$S(q_x, q_y) = \delta(q_x - \pi m)\delta(q_y - 2\pi n)\tfrac{1}{2}\big[1 + \cos q_x \cos(2\phi)\big] \tag{2.11}$$

with ϕ given by (2.6); m, n are two integers. If we consider the first Brillouin zone of the underlying lattice, the Bragg peaks are located at the zone centre, at the helix wave vector $q = (4\pi/5, 0)$, and at $q = (2\pi/5, 0)$ when the magnetic unit cell has five spins, whereas the peaks are located at the zone centre and at $q = (\pi, 0)$ in the spin-flop phase, as clearly shown by (2.10) and (2.11), respectively. In table 2 we give the intensity of the peaks as a function of the magnetic field. Note that the peak at $q = (2\pi/5, 0)$ is very weak over the whole range of fields and is rigorously zero for the regular helix configuration ($h = 0$). The peak at the zone centre, which is the square of the uniform magnetization, increases from zero to unity at increasing magnetic field. Like the magnetization, the intensity of the central peak undergoes two discontinuities at $h = h_1 = 0.334$ (distorted-helix–spin-flop transition) and at $h = h_2 = 1.419$ (spin-flop–fan transition). The intensity jumps, however, are small (0.018 at $h = h_1$ and 0.017 at $h = h_2$). The striking result is that the peak at the zone boundary in the spin-flop phase is replaced by a new peak at the helix wave vector in the helix or fan phase. At the transition coexistence of the two peaks should be found. Other useful parameters that can reveal the transition are the order parameters introduced in [10] for the triangular lattice and extended in [8] to the present lattice. They read

$$|\langle\psi_\parallel\rangle| = \frac{1}{5}\Big|\sum_{s=1}^{5} e^{i(s-1)4\pi/5}\cos\phi_s\Big| \tag{2.12}$$

$$|\langle\psi_\perp\rangle| = \frac{1}{5}\Big|\sum_{s=1}^{5} e^{i(s-1)4\pi/5}\sin\phi_s\Big|. \tag{2.13}$$

These parameters are suitable for describing a 'staggered magnetization' in the helix or fan phase. They vanish in the spin-flop phase. The dramatic effect on these parameters caused by the occurrence of the spin-flop phase is shown by the continuous curves of figure 5. Dotted curves show the same parameters when the transition to the spin-flop phase is ignored.

In order to support our suggestion about the occurrence of the spin-flop phase in the intermediate range of h for large enough Q we have investigated the helix with $Q = 6\pi/7$ which is stable at zero field and zero temperature on the line $1 + 2j_2 = -4j_3\cos 6\pi/7$. The energy for the configuration with seven spins per unit magnetic cell reads

$$e_0^{(H)} = -\tfrac{1}{7}\Big\{(1 + 2j_2)\,[2\cos\phi_2 + 2\cos(\phi_2 - \phi_3) + 2\cos(\phi_3 - \phi_4) + \cos(2\phi_4)]$$
$$+ 7(1 + j_3) + j_3\,[2\cos\phi_3 + 2\cos(\phi_2 - \phi_4) + 2\cos(\phi_3 + \phi_4) + \cos(2\phi_2)]$$
$$+ h(1 + 2\cos\phi_2 + 2\cos\phi_3 + 2\cos\phi_4)\Big\} \tag{2.14}$$

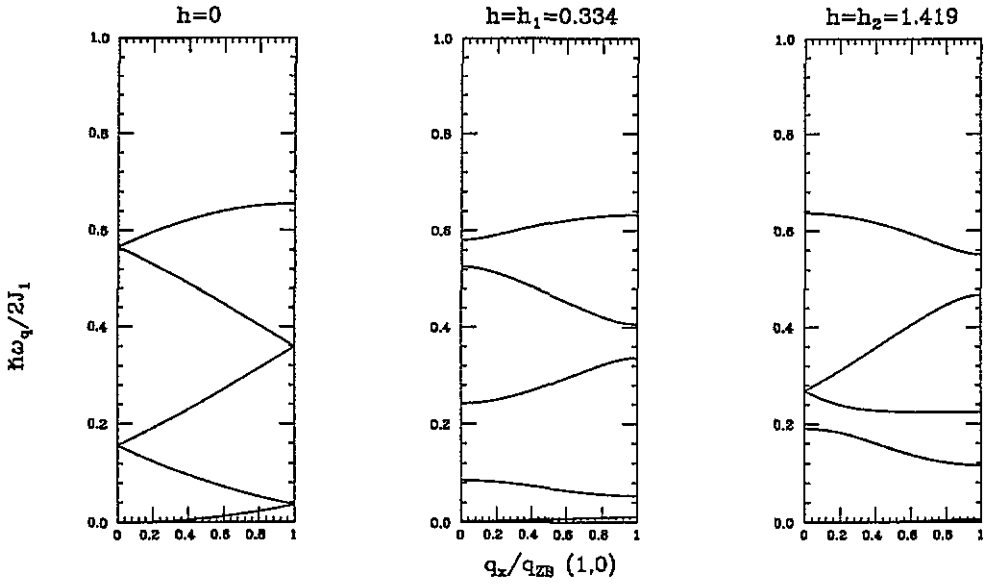

Figure 3. The dispersion curve in the (1,0) direction for the helix and fan phases for $h = 0$, $h = h_1 = 0.334$, and $h = h_2 = 1.419$.

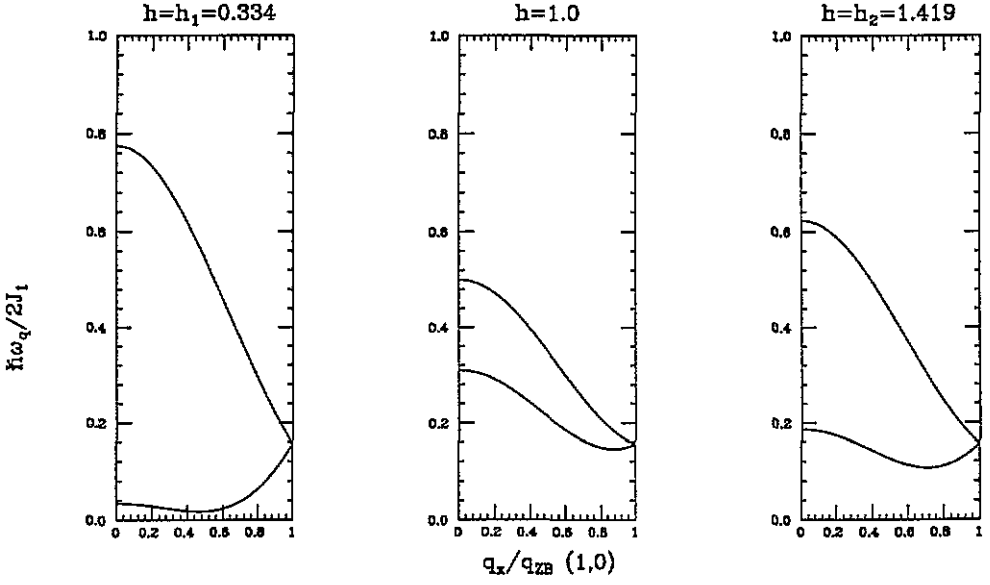

Figure 4. The dispersion curve in the (1,0) direction for the spin-flop phase for $h = h_1 = 0.334$, $h = 1$, and $h = h_2 = 1.419$.

where $\phi_1 = 0$, $\phi_2 = -\phi_7$, $\phi_3 = -\phi_6$, $\phi_4 = -\phi_5$ are the angles the seven spins of the unit cell make with the field. ϕ_2, ϕ_3, ϕ_4 are obtained by solving numerically the following equations:

$$(1 + 2j_2)[\sin\phi_2 + \sin(\phi_2 - \phi_3)] + j_3[\sin(\phi_2 - \phi_4) + \sin(2\phi_2)] + h\sin\phi_2 = 0 \qquad (2.15)$$

Table 2. Bragg peak intensity as a function of the magnetic field for $j_3 = -\frac{1}{8}$.

h	$S(0,0)$	$S(2\pi/5,0)$	$S(4\pi/5,0)$	$S(\pi,0)$
0	0	0	0.5	0
0.1	0.00197	0.00098	0.49804	0
0.2	0.00807	0.00393	0.49203	0
0.3	0.01938	0.00896	0.48135	0
0.4	0.06112	0	0	0.93889
0.5	0.09549	0	0	0.90451
0.6	0.13751	0	0	0.86249
0.7	0.18716	0	0	0.81284
0.8	0.24446	0	0	0.75554
0.9	0.30939	0	0	0.69061
1.0	0.38197	0	0	0.61803
1.1	0.46218	0	0	0.53782
1.2	0.55003	0	0	0.44997
1.3	0.64552	0	0	0.35448
1.4	0.74865	0	0	0.25135
1.5	0.86376	0.00120	0.06692	0
1.6	0.96304	0.00009	0.01840	0
1.6363	1	0	0	0

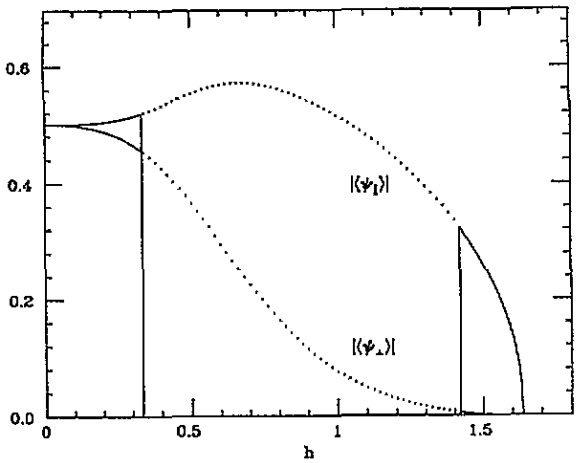

Figure 5. The order parameters as given by (2.12) and (2.13) at $T = 0$: actual result, continuous curve; the shape of the same parameters in the absence of the spin-flop transition, dotted curve.

$$(1+2j_2)\,[\sin(\phi_3-\phi_2)+\sin(\phi_3-\phi_4)]+j_3\,[\sin\phi_3+\sin(\phi_3+\phi_4)]+h\sin\phi_3=0 \quad (2.16)$$

$$(1+2j_2)\,[\sin(2\phi_4)+\sin(\phi_4-\phi_3)]+j_3\,[\sin(\phi_4-\phi_2)+\sin(\phi_4+\phi_3)]+h\sin\phi_4=0. \quad (2.17)$$

In table 3 we give the energy (2.14) for the helix with seven spins per cell and the energy (2.5) for the spin-flop phase with $j_3 = -0.125$. As one can see the spin-flop phase intervenes in the range $0.152 < h < 1.767$. The jumps in the magnetization are 0.032 and 0.002, respectively. This result strongly suggests that the behaviour we have found for $Q = 4\pi/5$ is not an accident when Q is large enough.

Table 3. A comparison between the energy ($e_0^{(H)}$) of the helix phase with seven spins per unit cell and the energy ($e_0^{(SF)}$) of the spin-flop phase as a function of the external magnetic field for $j_3 = -\frac{1}{8}$.

h	$e_0^{(H)}$	$e_0^{(SF)}$
0	−1.202 936	−1.200 484
0.1	−1.204 634	−1.203 259
0.2	−1.209 916	−1.211 584
0.3	−1.219 450	−1.225 546
0.4	−1.234 402	−1.244 881
0.5	−1.255 834	−1.269 854
0.6	−1.284 234	−1.300 377
0.7	−1.319 606	−1.336 449
0.8	−1.361 686	−1.378 071
0.9	−1.410 126	−1.425 242
1.0	−1.464 605	−1.477 963
1.1	−1.524 888	−1.536 234
1.2	−1.590 819	−1.600 054
1.3	−1.662 301	−1.669 424
1.4	−1.739 259	−1.744 343
1.5	−1.821 618	−1.824 812
1.6	−1.909 270	−1.910 831
1.7	−2.002 023	−2.002 399
1.8	−2.099 525	−2.099 517
1.8068	−2.106 357	−2.106 357

3. Monte Carlo simulation

In figure 2 diamonds and crosses show the uniform magnetization m_0 for $T = 0.2$ and $T = 0.35$, respectively, as obtained by a MC simulation on a sample of 25×25 spins with periodic boundary conditions. The initial 10^4 MC steps are discarded for thermalization, then runs of 10^4 MC steps have been made for any value of the magnetic field. As one can see the direct observation by MC simulation at finite temperature of the magnetization jumps obtained analytically at $T = 0$ is hopeless. However, we can obtain the signature of the distorted-helix–spin-flop phase transition evaluating the static structure factor by MC simulation on a sample of 50×50 spins, where the initial 4×10^4 MC steps have been discarded for thermalization, and runs of 2×10^4 MC steps are performed to obtain the static structure factor. In figure 6 the change of the magnetic cell when the magnetic field is increased from $h = 0.3$ to $h = 0.5$ is shown at $T = 0.05$. The transfer of weight from the peak at $q = (4\pi/5, 0)$ to $q = (\pi, 0)$ is clearly seen as expected on the basis of the results obtained at $T = 0$ in section 2. We stress that the occurrence of the spin-flop phase is indicated by the appearance of the peak at $q = (\pi, 0)$ to coincide with the disappearance of the peak at $q = (4\pi/5, 0)$. No discontinuity in the magnetization can be observed at temperature $T = 0.05$. Indeed the square root of the intensity of the peak at $q = (0, 0)$, that is, the uniform magnetization, changes continuously also for the 50×50 spin sample.

In principle an analogous phenomenon should occur when the field is changed from, say, $h = 1.4$ to $h = 1.5$, because a first order spin-flop–fan phase transition occurs at $T = 0$. However in this range of fields the substantial peak is at $q = 0$ because the spins are nearly collinear and the magnetization is almost saturated. Moreover thermal fluctuations make hard to pick out the modulation of the five spins in the unit cell of the helix phase as well as that of the two spins in the unit cell of the spin-flop phase. As one can see from table 2,

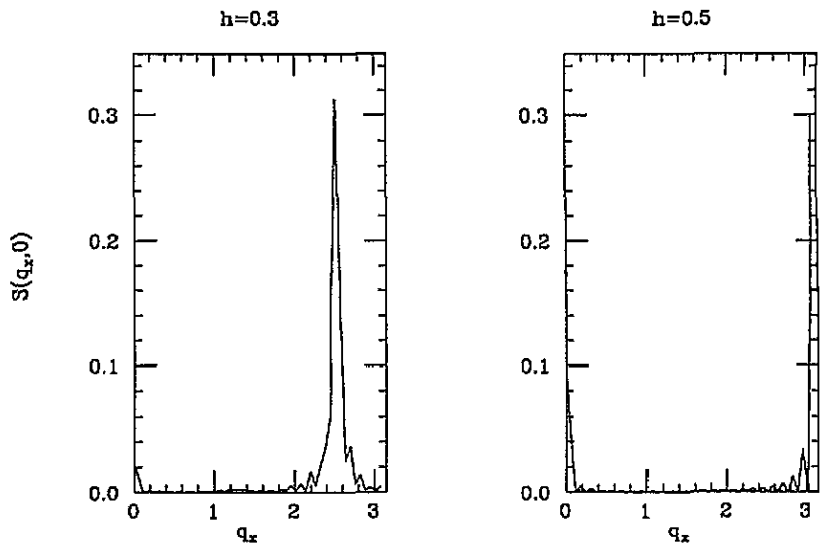

Figure 6. The static structure factor $S(q_x, 0)$ at $T = 0.05$ for $h = 0.3$ (helix phase) and $h = 0.5$ (spin-flop phase).

even at $T = 0$ the intensities of the peaks at $q = (4\pi/5, 0)$ and at $q = (\pi, 0)$ appear to be very weak.

4. Summary and conclusions

We have shown that a magnetic field induces discontinuous phase transitions between modulated spin configurations with different magnetic cells in continuous symmetry spin models. In particular, we have found this phenomenon in a square planar model with competing interactions up to third-nearest neighbours when the zero-field–zero-temperature configuration is a helix characterized by a wave vector $Q = (\frac{4}{5}\pi, 0)$. Indeed we have found that the elementary excitation energy of the distorted helix and fan configurations becomes negative at the zone boundary in an intermediate range of magnetic fields. This is the signature of the occurrence of an intermediate phase with two spins per unit cell, which we have identified as a spin-flop phase. This fact escaped a previous analysis based on the evaluation of the zero temperature energy of the model with the assumption that the size of the unit cell was unaffected by the field [6]. This approach suggests a first-order helix–fan phase transition when $Q < \pi/2$, and a continuous distortion from the low-field helix to the high-field fan configuration when $Q > \pi/2$. Since MC simulations were performed on a 2D sample of 25×25 spins [8] not suitable for describing dimerized phases and at too high a temperature, we carefully re-examined such numerical calculations and found a trace of the spin-flop phase in the static structure factor, performing an MC simulation on a sample of 50×50 spins as shown in figure 6. However, no evidence of the spin-flop phase is found in the uniform magnetization as a function of the field (see figure 2) where the discontinuities are small even at zero temperature. We stress that the scenario we find for $Q = 4\pi/5$, that is the existence of three commensurate phases before reaching the saturated phase, is qualitatively similar to that found in the planar triangular antiferromagnet [9–11] and in the square lattice with proper competing interactions [12], where distorted-helix, 'up–up–down',

and asymmetric fan configurations exist in addition to the saturated phase [9–11]. However, the intermediate up–up–down phase is stabilized only by thermal fluctuations whereas the spin-flop phase is present even at zero temperature over a wide range of magnetic fields in the model we consider here. We think that the occurrence of the spin-flop phase in the intermediate range of fields should be a general rule of the helix configuration with large enough Q. Indeed we have studied the minimum-energy configuration at zero temperature for exchange competition supporting a magnetic cell with seven spins in the square planar model. The discontinuous transition from the $Q = 6\pi/7$ helix to the spin flop phase and from the latter to the symmetric fan is confirmed.

Appendix

When small deviations from the minimum-energy configurations are accounted for in Hamiltonian (2.1), we obtain an expansion in which $\mathcal{H}_n$ contains the product of n deviations. The zero order term is the minimum-energy configuration. The first-order term vanishes because of the minimum conditions. If we restrict ourselves to the second-order term (harmonic approximation) we have

$$\mathcal{H} = \mathcal{H}_0 + \mathcal{H}_2 \tag{A1}$$

where

$$\mathcal{H}_0 = E_0^{(\mathrm{H})} \tag{A2}$$

$$\mathcal{H}_2 = 2J_1 \sum_{s,s'=1}^{5} \sum_{q} \psi_{-q}^{(s)} A_q^{ss'} \psi_q^{(s')} \tag{A3}$$

for the five-sublattice helix or fan configuration, and

$$\mathcal{H}_0 = E_0^{(\mathrm{SF})} \tag{A4}$$

$$\mathcal{H}_2 = 2J_1 \sum_{s,s'=1}^{2} \sum_{q} \psi_{-q}^{(s)} B_q^{ss'} \psi_q^{(s')} \tag{A5}$$

for the spin-flop phase. $\psi_q^{(s)}$ are the spatial Fourier transforms of $\psi_i^{(s)}$, which are the small deviations the sth spin in the ith magnetic cell makes with respect to the minimum-energy configuration. $E_0^{(\mathrm{H})}$ and $E_0^{(\mathrm{SF})}$ are given by (2.4) and (2.5), respectively.

The elements $A_q^{ss'}$ of the hermitian matrix $\mathbf{A}_q$ are given by

$$A_q^{11} = 1 - \cos q_y + j_3(\sqrt{5}+1)\cos\phi_2 + j_3\left[1 - \cos(2q_y) + \cos\phi_3\right] + \frac{h}{2} \tag{A6}$$

$$A_q^{22} = 1 - \cos q_y + \tfrac{1}{2} j_3(\sqrt{5}+1)\left[\cos(\phi_2 - \phi_3) + \cos\phi_2\right] + j_3\left\{1 - \cos(2q_y) + \tfrac{1}{2}\left[\cos(\phi_2 + \phi_3) + \cos(2\phi_2)\right]\right\} + \frac{h}{2}\cos\phi_2 \tag{A7}$$

$$A_q^{33} = 1 - \cos q_y + \tfrac{1}{2} j_3(\sqrt{5}+1)\left[\cos(\phi_2 - \phi_3) + \cos(2\phi_3)\right] + j_3\left\{1 - \cos(2q_y) + \tfrac{1}{2}\left[\cos(\phi_2 + \phi_3) + \cos\phi_3\right]\right\} + \frac{h}{2}\cos\phi_3 \tag{A8}$$

$$A_q^{44} = A_q^{33} \tag{A9}$$

$$A_q^{55} = A_q^{22} \tag{A10}$$

$$A_q^{12} = -\tfrac{1}{2}e^{iq_x}\cos\phi_2\left[1 - \cos q_y + j_3(\sqrt{5}+1)\cos q_y\right] \tag{A11}$$

$$A_q^{13} = -\tfrac{1}{2}e^{2iq_x} j_3 \cos\phi_3 \tag{A12}$$

$$A_q^{14} = (A_q^{13})^* \tag{A13}$$

$$A_q^{15} = (A_q^{12})^* \tag{A14}$$

$$A_q^{23} = -\tfrac{1}{2}e^{iq_x}\cos(\phi_2 - \phi_3)\left[1 - \cos q_y + j_3(\sqrt{5}+1)\cos q_y\right] \tag{A15}$$

$$A_q^{24} = -\tfrac{1}{2}e^{2iq_x} j_3 \cos(\phi_2 + \phi_3) \tag{A16}$$

$$A_q^{25} = -\tfrac{1}{2}e^{-2iq_x} j_3 \cos(2\phi_2) \tag{A17}$$

$$A_q^{34} = -\tfrac{1}{2}e^{iq_x}\cos(2\phi_3)\left[1 - \cos q_y + j_3(\sqrt{5}+1)\cos q_y\right] \tag{A18}$$

$$A_q^{35} = A_q^{24} \tag{A19}$$

$$A_q^{45} = A_q^{23} \tag{A20}$$

where ϕ_2 and ϕ_3 are the solutions of (2.2) and (2.3).

The elements $B_q^{ss'}$ of the hermitian matrix $\mathbf{B}_q$ are given by

$$B_q^{11} = 1 - \cos q_y - j_3(\sqrt{5}+1) + j_3\left[2 - \cos(2q_x) - \cos(2q_y)\right] \tag{A21}$$

$$B_q^{12} = -\cos(2\phi)\cos q_x\left[1 - \cos q_y + j_3(\sqrt{5}+1)\cos q_y\right] \tag{A22}$$

where ϕ is given by (2.6). The elementary excitation energies are given by

$$\hbar\omega_q = 2J_1\lambda_q^{(s)} \tag{A23}$$

where λ_q are the eigenvalues of the matrix $\mathbf{A}_q$ for the helix phase and of the matrix $\mathbf{B}_q$ for the spin-flop phase. Five branches are found in the first Brillouin zone of the helix or fan phase ($0 < q_x < \pi/5$, $0 < q_y < \pi$); two branches are found in the first Brillouin zone of the spin-flop phase ($0 < q_x < \pi/2$, $0 < q_y < \pi$).

References

[1] Fisher M E and Selke W 1980 *Phys. Rev. Lett.* **44** 1502
[2] Rastelli E, Tassi A and Reatto L 1979 *Physica* B **97** 1
[3] Rastelli E and Tassi A 1986 *J. Phys. C: Solid State Phys.* **19** L423
[4] Villain J 1959 *J. Phys. Chem. Solids* **11** 303
Yoshimori J 1959 *J. Phys. Soc. Japan* **14** 807
Kaplan T A 1959 *Phys. Rev.* **116** 888
[5] Harris A B, Rastelli E and Tassi A 1991 *Phys. Rev.* B**44** 2624
[6] Rastelli E, Tassi A, Melegari G and Pimpinelli A 1992 *J. Magn. Magn. Mater.* **104** 173
[7] Carazza B, Rastelli E and Tassi A 1991 Z. *Phys.* B **84** 301
[8] Rastelli E, Sedazzari S and Tassi A 1993 *J. Phys.: Condens. Matter* **5** 7121
[9] Kawamura H 1984 *J. Phys. Soc. Japan* **53** 2452
[10] Lee D H, Joannopoulos J D, Negele J W and Landau D P 1984 *Phys. Rev. Lett.* **52** 433; 1986 *Phys. Rev.* B **33** 450
[11] Rastelli E, Tassi A, Pimpinelli A and Sedazzari S 1992 *Phys. Rev.* B **45** 7936
[12] Gallanti C, Rastelli E, Sedazzari S and Tassi A 1993 *J. Appl. Phys.* **73** 5482